PHYSICAL REVIEW B **81**, 201102(R) (2010)

Strong orbital polarization in orthorhombic $DyMnO_3$: A combined x-ray linear dichroism and *ab initio* electronic structure study

J. M. Chen,[1,*,†] Z. Hu,[2,3,*,‡] H. T. Jeng,[4] Y. Y. Chin,[2,3] J. M. Lee,[1,5] S. W. Huang,[1,5] K. T. Lu,[1] C. K. Chen,[1] S. C. Haw,[1] T. L. Chou,[1] H.-J. Lin,[1] C. C. Shen,[6] R. S. Liu,[6] A. Tanaka,[7] L. H. Tjeng,[2,3] and C. T. Chen[1]

[1]*National Synchrotron Radiation Research Center, Hsinchu 30076, Taiwan, Republic of China*

[2]*Max Planck Institute for Chemical Physics of Solids, 01187 Dresden, Germany*

[3]*II. Physikalisches Institut, Universität zu Köln, D-50937 Köln, Germany*

[4]*Institute of Physics, Academia Sinica, Taipei 11529, Taiwan, Republic of China*

[5]*Department of Electrophysics, National Chiao Tung University, Hsinchu 30010, Taiwan, Republic of China*

[6]*Department of Chemistry, National Taiwan University, Taipei 10617, Taiwan, Republic of China*

[7]*Department of Quantum Matter, ADSM, Hiroshima University, Higashi-Hiroshima 739-8526, Japan*

(Received 21 March 2010; revised manuscript received 6 May 2010; published 26 May 2010)

We present a combined experimental and theoretical study on the Mn 3*d* orbital occupation in orthorhombic $DyMnO_3$ single crystals. We have observed a very strong polarization dependence in the Mn $L_{2,3}$ x-ray absorption spectra, indicative for a distinct anisotropic orbital occupation. *Ab initio* electronic-structure calculations clearly infer the existence of a strong orbital polarization in the e_g band with a staggered $d_{3x^2-r^2}/d_{3y^2-r^2}$-type ordering pattern in the *ab* plane. This finding is in excellent agreement with a quantitative analyis of the spectra using the atomic multiplet cluster approach.

DOI: 10.1103/PhysRevB.81.201102 PACS number(s): 78.70.Dm, 77.84.−s, 71.70.Ch, 75.50.Ee

Correlated-electron materials such as the 3*d* transition-metal (TM) oxides exhibit an exceptionally rich variety of physical properties. These include, for example, metal-insulator transitions (MIT), colossal magnetoresistance, superconductivity, and multiferroicity. It is well recognized by now that the anisotropy in the TM 3*d* orbital occupation is a key factor for the extraordinary magnetic and electronic properties since it is intricately coupled to the charge, spin, and lattice dynamics.[1–7] The MIT in VO_2, V_2O_3, and Ca_2RuO_4 was found to be associated with a redistribution of the orbital occupation.[8–10] The occupation of the d_2 and d_0d_2 orbitals with minority spin gives rise to a giant orbital moment about $2\mu_B$ for $Ca_3Co_2O_6$ and Ca_3CoRhO_6, respectively, elucidating the highly Ising-type magnetism.[11,12] It was found that in CoO thin films the magnetic moments are oriented out of plane if the t_{2g} hole is situated in an orbital characterized by a linear combination of the d_{xz} and d_{yz} states and in plane if it is in the d_{xy} orbital.[13] In $LiVO_2$, it was found that orbital ordering removes the spin frustration in the triangular lattice and drives the system into a spin-singlet state without any long-range magnetic order.[14] In the manganese oxides, the orbital and charge ordering plays an important role for the colossal magnetoresistance and the metal-insulator transition.[1,15] On top of this, orbital order could also lead to ferroelectricity.[4,5,7]

In the $RMnO_3$ (R=rare earth) system, the high-spin Mn ion has the $t_{2g}^3e_g^1$ configuration. A strong Jahn-Teller (JT) distortion occurs to lift the degeneracy in the e_g orbital and leads to a pattern of orbital ordering through the crystal lattice. The spin ordering is coupled to the ordered orbital pattern according to the Goodenough-Kanamori rules.[16,17] The different displacements of the oxygen ions around the Mn ions in $RMnO_3$ (R=Tb, Dy, and Gd) causes strong distortions and tilting of the MnO_6 octahedra as well as a reduction in Mn-O-Mn bond angles, thereby yielding a complicated pattern of orbital and spin ordering, which in turn is thought of as the origin of the observed ferroelectricity.[7,18–20] Thus, orbital polarization and ordering in orthorhombic $RMnO_3$ (R=Tb, Dy, and Gd) is an indispensable ingredient for the formation of complicated incommensurate spin structures at low temperatures.

Indeed, it was found recently that the Mn $L_{2,3}$-edge x-ray absorption spectra of hexagonal $YMnO_3$ and $DyMnO_3$ exhibit a strong polarization dependence, indicative for the presence of distinct orbital occupations in the e_g subshell. Yet, it is quite puzzling that such polarization dependence was not observed in the study on orthorhombic $DyMnO_3$.[21,22] We note that thin films were used in that study. Our objective is now to resolve this issue and to reinvestigated the orbital occupations of the Mn 3*d* states in orthorhombic $DyMnO_3$ using bulk single crystals.

Polarization-dependent x-ray absorption spectroscopy (XAS) at the 3*d* TM $L_{2,3}$ edge, complemented with multiplet cluster calculations, is a powerful method to determine the 3*d* orbital occupation in transition-metal oxides[8,9,13,23] and have provided information of orbital ordering pattern in $La_{1-x}Sr_xMnO_3$ and $La_{2-x}Sr_xMnO_4$.[24–29]

In this Rapid Communication, we carried out our XAS study on orthorhombic $DyMnO_3$ single crystals using three independent polarizations, namely, $E\|a$, $E\|b$, and $E\|c$, where E denotes the electric field vector and a,b,c the crystallographic directions of orthorhombic $DyMnO_3$. In contrast with the results of previous experiments, we found that the Mn $L_{2,3}$ x-ray absorption spectra of orthorhombic $DyMnO_3$ single crystals do show a strong polarization dependence. We also performed *ab initio* band-structure calculations and obtained a strong zigzag e_g orbital polarization in the *ab* plane with the $d_{3x^2-r^2}$ (or $d_{3y^2-r^2}$) orbital occupation number close to 1. The corresponding orbital polarization is in excellent agreement with the analysis of the experimental spectra using the multiplet cluster calculations.

Untwined high-quality orthorhombic $DyMnO_3$ single crystals (space group: *Pbnm*) were grown by the high-temperature solution method with a PbF_2 flux in a Pt crucible. The rocking curve of the $DyMnO_3$ crystal has the full width at half maximum of ~0.01° for the (0 0 2) Bragg reflection, indicating the excellent crystal quality. Two crystal surfaces with crystallographic directions of (100), (010) (i.e., *ab* plane) and (100), (001) (i.e., *ac* plane), respectively, were aligned using an x-ray diffractometer. Total electron-yield Mn $L_{2,3}$-edge x-ray absorption spectra, with a photon energy resolution of ~0.16 eV at 642 eV, were recorded at the Dragon beamline at National Synchrotron Radiation Research Center in Taiwan. The degree of linear polarization of the incident light was ~99%. The crystals were mounted with the surface normal parallel to the Poynting vector of the light. Clean crystal surfaces were obtained by cleaving the crystals *in situ* in an ultrahigh-vacuum chamber with a base pressure $\sim 5\times 10^{-10}$ Torr. A MnO single crystal was measured simultaneously in a separate chamber, which enabled us to achieve better than 0.02 eV accuracy in the relative energy alignment. Different $DyMnO_3$ crystals with the same axis showed excellent reproducibility of the experimental spectra, indicating the high quality of our crystals.

We performed band-structure calculations in a generalized gradient approximation plus on-site Coulomb interaction U (GGA+U) for A-type antiferromagnetic (AFM) structures of $DyMnO_3$. The band-structure calculations were performed using the full-potential projected augmented wave method as implemented in the Vienna *ab initio* simulation package (VASP). In the GGA+U calculations, a Coulomb energy U=5.0 eV and an intra-atomic exchange parameter J=0.87 eV for the Mn 3*d* electrons were used.[30] The crystal-field potential due to the O^{2-} ligands within the $Mn^{3+}O_6$ octahedra in $DyMnO_3$ splits the fivefold Mn 3*d* orbitals into three lower-lying t_{2g} (d_{xy}, d_{yz}, and d_{xz}) orbitals and two higher-lying e_g orbitals. The e_g doublet is split further into two subbands $e_g^1\uparrow$ and $e_g^2\uparrow$ resulting from a strong JT distortion. Three *d* electrons are in the 1/2-filled t_{2g} shell and one in the e_g. The key issue is the distribution of this e_g electron between the in-plane $d_{3x^2-r^2}(d_{3y^2-r^2})$ and out-of-plane $d_{y^2-z^2}(d_{x^2-z^2})$ orbitals.

Figure 1(a) displays the orbital-projected partial density of states of fivefold Mn 3*d* states for $DyMnO_3$ using a local coordination on the Mn(4) site based on the GGA+U cacu-lations. There is a small indirect gap between the JT-split Mn $e_g^1\uparrow$ and $e_g^2\uparrow$ bands. Based on the GGA+U calculations, the occupied $e_g^1\uparrow$ and unoccupied $e_g^2\uparrow$ bands are dominated by $d_{3x^2-r^2}$ and $d_{y^2-z^2}$ orbitals, respectively, in one coplanar Mn ion, whereas they exhibit predominantly $d_{3y^2-r^2}$ and $d_{x^2-z^2}$ character, respectively, for the other coplanar Mn ion. Figure 1(b) shows the electronic valence charge-density contour on the basal plane of $DyMnO_3$. It clearly reveals the strong orbital polarization of the e_g band with a staggered $d_{3x^2-r^2}$ ($d_{3y^2-r^2}$)-type orbital ordering pattern in the *ab* plane.

Figure 2(a) shows our experimental polarization-dependent Mn $L_{2,3}$-edge absorption spectra of bulk $DyMnO_3$ single crystals for the three polarizations: $E\|a$ (red line), $E\|b$ (black line), and $E\|c$ (blue line). The experimental linear dichroic (LD) spectra, namely, the difference between two polarizations, i.e., $(E\|c)-(E\|a)$, $(E\|b)-(E\|c)$, and $(E\|b)-(E\|a)$ (green line) are depicted in Figs. 2(c)–2(e). It is clear that our spectra exhibit a very strong polarization dependence along the three different crystallographic directions in sharp contrast to the results of previous experiments on $DyMnO_3$ thin films which showed practically only isotropiclike spectra (possibly due to strain effect on substrates).[21,22] In our spectra, for example, the main peak for the $E\|b$ polarization (i.e., the direction of spiral spin) lies at a lower energy than for polarizations $E\|a$ and $E\|c$. Our spectra therefore, provide a clear indication for a large anisotropic orbital occupation of Mn e_g states as expected for the strongly distorted MnO_6 octahedron.[31]

To extract information on the orbital occupation from the polarization-dependent Mn $L_{2,3}$-edge XAS spectra of

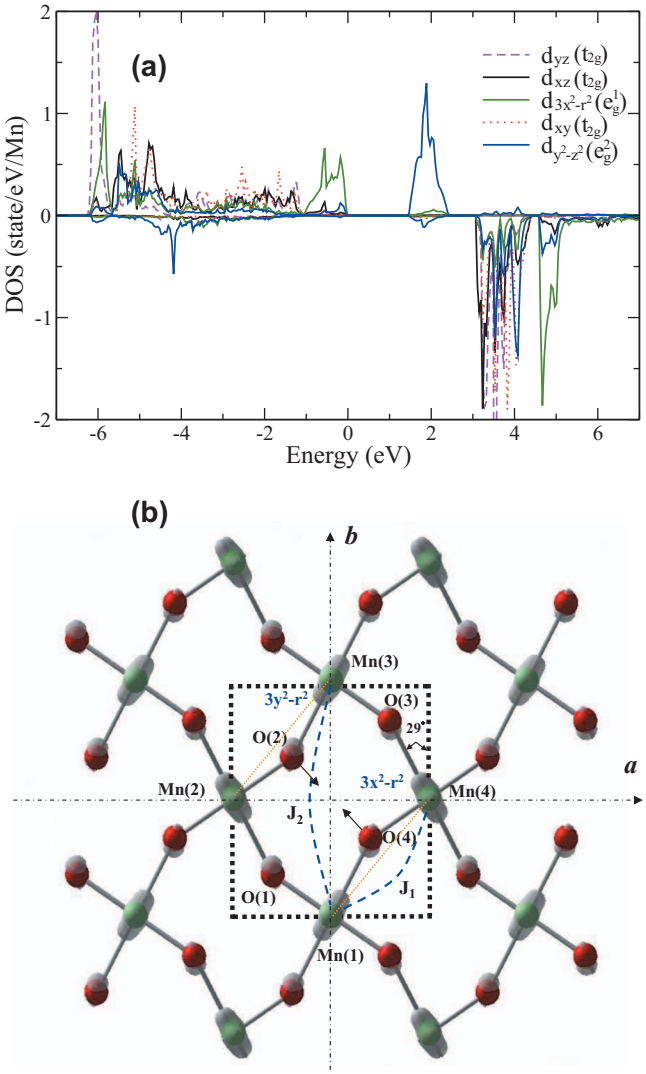

FIG. 1. (Color) (a) Orbital-projected partial density of states of fivefold Mn 3*d* states on the Mn(4) site for an A-type antiferromagnetic structure of orthorhombic $DyMnO_3$ calculated with the GGA+U method. The parameters in these calculations are described in the text. For each panel the upper half denotes the and the lower half the minority-spin states. The energy zero is at the Fermi energy (E_f). (b) Electronic valence charge-density contour plot on the basal plane of $DyMnO_3$.The green and red balls denote Mn and O ions, respectively. Gray lobes on Mn ions indicate occupied $e_g^1\uparrow$.

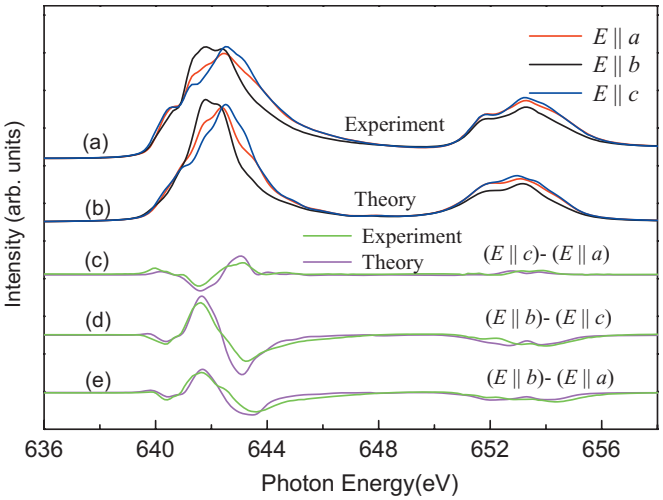

FIG. 2. (Color) (a) Experimental and (b) theoretical polarization-dependent Mn $L_{2,3}$-edge absorption spectra of single-crystalline $DyMnO_3$ for (a) $E\|a$ (red line), $E\|b$ (black line), and $E\|c$ (blue line). Experimental (green line) and theoretical (magenta line) LD spectra for $(E\|c)-(E\|a)$, $(E\|b)-(E\|c)$, and $(E\|b)-(E\|a)$ are shown in (c), (d), and (e), respectively.

$DyMnO_3$, we have simulated the experimental spectra using the well-proven cluster model.[32,33] The method uses for each Mn site a MnO_6 cluster which includes the full atomic multiplet theory and the local effects of the solid. It accounts for the intra-atomic 3*d*-3*d* and 2*p*-3*d* Coulomb interactions, the atomic 2*p* and 3*d* spin-orbit couplings, the O 2*p*-Mn 3*d* hybridization, and the proper local crystal-field parameters. The parameters for the multipole part of the Coulomb interactions were given by the Hartree-Fock values while the monopole parts $U_{cd}-U_{dd}=1.5$ eV and O 2*p*-Mn 3*d* charge-transfer energy $\Delta=4$ eV were estimated from photoemission experiments on $LaMnO_3$.[34] The Mn 3*d*-O 2*p* transfer integrals were adapted to account for the various Mn-O bond lengths according to Harrison's prescription.[35] The crystal splitting between e_g and t_{2g} states, $10Dq$, the splitting of e_g states, Δe_g, and the splitting of t_{2g} states, Δt_{2g}, are tuned to reproduce the experimental spectra.

The simulated spectra for the three polarizations $E\|a$ (red line), $E\|b$ (black line), and $E\|c$ (blue line) are given in Fig. 2(b). Figures 2(c)–2(e) show a comparison of the experimental (green line) with the theoretical LD spectra (magenta line). One can clearly see that we have been able to achieve a very good agreement between the simulation and the experiment. From this set of best fits we obtain values of 0.9 eV, 0.7 eV, and 0.2 eV for the crystal splitting parameters $10Dq$, Δe_g, and Δt_{2g}, respectively, and we have used $pd\sigma=-2.10$, -1.76 and -1.43 eV and $pd\pi=-pd\sigma/2.15$ for the three Mn-O bonds.

We have also extracted the orbital occupation numbers from the set of best simulations. These numbers are presented in Table I, where one can see the very large $d_{3x^2-r^2}$ orbital occupation number of 1.06. This is even larger than the 0.81 value in $LaMnO_3$.[36,37] The result demonstrates that the e_g electron is constrained to the $d_{3x^2-r^2}$ or $d_{3y^2-r^2}$ orbital. The small occupation number of 0.38 in $d_{y^2-z^2}$ orbital in Table I is originating from the Mn-O covalent mixing. The

TABLE I. Occupation numbers of Mn 3*d* states and ligand molecular orbitals on the Mn(4) site in orthorhombic $DyMnO_3$ deduced from configuration-interaction cluster simulation.

	$3x^2-r^2$	y^2-z^2	yz	zx	xy
Mn 3*d*	1.06	0.39	1.03	1.02	1.03
O 2*p*	1.92	1.64	1.97	1.98	1.97

negative integrals in the LD spectra $(E\|b)-(E\|a)$ and $(E\|b)-(E\|c)$ are indicative for a relatively large projection of the occupied $d_{3x^2-r^2}$ and $d_{3y^2-r^2}$ orbitals along the *b* direction. This is in good agreement with the orbital ordering pattern shown in Fig. 1(b), in which the angle between the $d_{3x^2-r^2}$ (or $d_{3y^2-r^2}$) and the *b* axis is 29° (40° in $LaMnO_3$), reflecting the significant $GdFeO_3$-type distortion and the decrease in the Mn-O-Mn bond angle.[38]

For the orbital polarization of the e_g-JT electron, the occupied e_g-orbital wave function is generally described as

$$\phi(\theta)=\cos(\theta/2)|3z^2-r^2\rangle \pm \sin(\theta/2)|x^2-y^2\rangle. \quad (1)$$

Here θ defines the respective orbital component.[3,39] The simplest case of an alternative $d_{3z^2-r^2}$ and $d_{x^2-y^2}$ ordering corresponds to $\theta=0°$ and 180°, respectively. The angle θ can be estimated from the actual magnitude of the JT distortion and is given by the expression

$$\tan(\theta)=\frac{\sqrt{3}(l-s)}{2m-l-s}, \quad (2)$$

here *l*, *m*, and *s* denote the three Mn-O unit distances.[3] We obtain a θ angle of ~113° for Mn-O distances of 2.24, 1.94, and 1.89 Å in orthorhombic $DyMnO_3$. This is close to the 120° scenario corresponding to a staggered $d_{3x^2-r^2}/d_{3y^2-r^2}$ type of orbital ordering, consistent with the present experimental results and GGA+*U* calculations. The larger differences between the three Mn-O distances in $DyMnO_3$ lead to the formation of a staggered $d_{3x^2-r^2}/d_{3y^2-r^2}$ type of orbital ordering as compared with the smaller differences in the Mn-O distances of 2.00, 1.98, and 1.84 Å in $La_{0.5}Sr_{1.5}MnO_4$ exhibiting a cross-type orbital ordering of $d_{x^2-z^2}/d_{y^2-z^2}$.[26]

As shown in Fig. 1(b), the distortion leads to a shorter distance between O_2 and O_4, which in turn slightly changes the next-nearest-neighbor (NNN) AFM superexchange interaction through the Mn(1)-O_4-O_2-Mn(3) paths (J_2 on the order of a few millielectron volts), since the occupied e_g orbitals in the Mn(1) and Mn(3) are parallel. At the same time, this distortion strongly suppresses the predominant NN ferromagnetic (FM) superexchange interaction ($J_1=-13$ meV for $LaMnO_3$ and ~−2 meV for $DyMnO_3$).[18,40] Under the staggered $d_{3x^2-r^2}/d_{3y^2-r^2}$ type of orbital ordering as shown in Fig. 1(b), the AFM NNN superexchange interaction between Mn(1) and Mn(3) (along the *b* axis) is stronger than that between Mn(2) and Mn(4) (along the *a* axis). Thus, a subtle balance of the competition between the NN FM and the NNN AFM superexchange interactions along the *b* axis leads to a frustrated spin system and gives rise to a noncollinear spin arrangement in the spiral phase at low temperatures.[18,19]

In conclusion, we have observed a strong polarization dependence in the soft-x-ray absorption spectra at the Mn $L_{2,3}$ edge in orthorhombic $DyMnO_3$ single crystals. *Ab initio* electronic-structure calculations clearly reveal a strong orbital polarization in the e_g band with a staggered $d_{3x^2-r^2}/d_{3y^2-r^2}$ type of ordering pattern in the *ab* plane. Configuration-interaction cluster calculations revealed that the e_g electron is indeed constrained to the $d_{3x^2-r^2}$ or $d_{3y^2-r^2}$ orbital. The negative integral intensity of linear dichroic spectra $(E\|b)-(E\|a)$ and $(E\|b)-(E\|c)$ points toward a relatively large projection of the occupied $d_{3x^2-r^2}$ and $d_{3y^2-r^2}$ orbitals along the *b* direction. The coexistence and competition between NN FM and NNN AFM interactions along the *b* axis lead to a frustrated spin system giving rise to the complex magnetic structure.

This research is supported by the NSRRC and the National Science Council of the Republic of China under Grant No. NSC 96-2113-M-213-007-MY3 and the research in Cologne is supported by the Deutsche Forschungsgemeinschaft under Grant No. SFB 608, and by the European Union through the ITN SOPRANO network.

*Author to whom all correspondence should be addressed.
†jmchen@nsrrc.org.tw
‡zhiwei.hu@cpfs.mgp.de

[1] Y. Tokura and N. Nagaosa, Science **288**, 462 (2000).
[2] B. Keimer and A. M. Oles, New J. Phys. **6**, E05 (2004).
[3] D. I. Khomskii, Phys. Scr. **72**, CC8 (2005).
[4] B. Keimer, Nature Mater. **5**, 933 (2006).
[5] Y. Tokunaga *et al.*, Nature Mater. **5**, 937 (2006).
[6] E. Dagotto and Y. Tokura, MRS Bull. **33**, 1037 (2008).
[7] K. Yamauchi and S. Picozzi, J. Phys.: Condens. Matter **21**, 064203 (2009).
[8] M. W. Haverkort *et al.*, Phys. Rev. Lett. **95**, 196404 (2005).
[9] J.-H. Park, L. H. Tjeng, A. Tanaka, J. W. Allen, C. T. Chen, P. Metcalf, J. M. Honig, F. M. F. de Groot, and G. A. Sawatzky, Phys. Rev. B **61**, 11506 (2000).
[10] T. Mizokawa, L. H. Tjeng, G. A. Sawatzky, G. Ghiringhelli, O. Tjernberg, N. B. Brookes, H. Fukazawa, S. Nakatsuji, and Y. Maeno, Phys. Rev. Lett. **87**, 077202 (2001).
[11] T. Burnus *et al.*, Phys. Rev. B **74**, 245111 (2006).
[12] T. Burnus *et al.*, Phys. Rev. B **77**, 205111 (2008).
[13] S. I. Csiszar, M. W. Haverkort, Z. Hu, A. Tanaka, H. H. Hsieh, H. J. Lin, C. T. Chen, T. Hibma, and L. H. Tjeng, Phys. Rev. Lett. **95**, 187205 (2005).
[14] H. F. Pen, J. van den Brink, D. I. Khomskii, and G. A. Sawatzky, Phys. Rev. Lett. **78**, 1323 (1997).
[15] B. B. Van Aken, O. D. Jurchescu, A. Meetsma, Y. Tomioka, Y. Tokura, and T. T. M. Palstra, Phys. Rev. Lett. **90**, 066403 (2003).
[16] J. B. Goodenough, Phys. Rev. **100**, 564 (1955).
[17] J. Kanamori, J. Phys. Chem. Solids **10**, 87 (1959).
[18] T. Kimura, S. Ishihara, H. Shintani, T. Arima, K. T. Takahashi, K. Ishizaka, and Y. Tokura, Phys. Rev. B **68**, 060403(R) (2003).
[19] D. Senff, P. Link, K. Hradil, A. Hiess, L. P. Regnault, Y. Sidis, N. Aliouane, D. N. Argyriou, and M. Braden, Phys. Rev. Lett. **98**, 137206 (2007).
[20] N. Aliouane, K. Schmalzl, D. Senff, A. Maljuk, K. Prokes, M. Braden, and D. N. Argyriou, Phys. Rev. Lett. **102**, 207205 (2009).
[21] D.-Y. Cho *et al.*, Phys. Rev. Lett. **98**, 217601 (2007).
[22] D.-Y. Cho, S. J. Oh, D. G. Kim, A. Tanaka, and J. H. Park, Phys. Rev. B **79**, 035116 (2009).
[23] F. Iga *et al.*, Phys. Rev. Lett. **93**, 257207 (2004).
[24] A. Tebano *et al.*, Phys. Rev. Lett. **100**, 137401 (2008).
[25] M. Huijben, L. W. Martin, Y. H. Chu, M. B. Holcomb, P. Yu, G. Rijnders, D. H. A. Blank, and R. Ramesh, Phys. Rev. B **78**, 094413 (2008).
[26] D. J. Huang *et al.*, Phys. Rev. Lett. **92**, 087202 (2004).
[27] J. Chakhalian *et al.*, Science **318**, 1114 (2007).
[28] M. Merz *et al.*, Eur. Phys. J. B **51**, 315 (2006).
[29] V. R. Galakhov, M. C. Falub, K. Kuepper, and M. Neumann, J. Struct. Chem. **49**, 54 (2008).
[30] G. Giovannetti and J. van den Brink, Phys. Rev. Lett. **100**, 227603 (2008).
[31] J. M. Chen *et al.*, Phys. Rev. B **79**, 165110 (2009).
[32] A. Tanaka and T. Jo, J. Phys. Soc. Jpn. **63**, 2788 (1994).
[33] F. M. F. de Groot, J. Electron Spectrosc. Relat. Phenom. **67**, 529 (1994).
[34] A. E. Bocquet, T. Mizokawa, T. Saitoh, H. Namatame, and A. Fujimori, Phys. Rev. B **46**, 3771 (1992).
[35] W. A. Harrison, *Electronic Structure and the Properties of Solids* (Dover, New York, 1989).
[36] J. E. Medvedeva, M. A. Korotin, V. I. Anisimov, and A. J. Freeman, Phys. Rev. B **65**, 172413 (2002).
[37] W. Luo, A. Franceschetti, M. Varela, J. Tao, S. J. Pennycook, and S. T. Pantelides, Phys. Rev. Lett. **99**, 036402 (2007).
[38] S.-G. Eriksson *et al.*, Mater. Sci. Forum **378-381**, 505 (2001).
[39] K. Tobe, T. Kimura, Y. Okimoto, and Y. Tokura, Phys. Rev. B **64**, 184421 (2001).
[40] K. Yamauchi, F. Freimuth, S. Blugel, and S. Picozzi, Phys. Rev. B **78**, 014403 (2008).